para-Functionalized NCN-Pincer Palladium(II) Complexes: Synthesis, Catalysis and DFT Calculations

Harm P. Dijkstra,[a] Martijn Q. Slagt,[a] Aidan McDonald,[a] Cornelis A. Kruithof,[a] Robert Kreiter,[a] Allison M. Mills,[b] Martin Lutz,[b] Anthony L. Spek,[b][‡] Wim Klopper,[c][‡‡] Gerard P. M. van Klink,[a] and Gerard van Koten*[a]

Keywords: Density functional calculations / Homogeneous catalysis / Substituent effects / Supported catalysts / Synthesis design

Several *para*-substituted NCN-pincer palladium(II) complexes (**1a**–**g** and **6a**–**g**) {NCN = $[C_6H_3(CH_2NMe_2)_2$-2,6$]^-$, *para* = 4-position} have been prepared and the electronic influences of the *para* substituents were studied in catalysis as well as by DFT calculations (B3LYP/LANL2DZ). From DFT calculations, it was found that the *para* substituent exerts only a minor effect on the partial charge, investigated by means of the Mulliken population analysis, at the palladium(II) center. Also, when the *para*-functionalized, cationic NCN–Pd^{II} complexes **6a**–**g** were applied as Lewis acid catalysts in the double Michael reaction between methyl vinyl ketone and ethyl α-cyanoacetate, only small differences in the activities of the various catalysts were observed. These results, when translated to immobilized multipincer catalysts, imply that various *para* functionalities can be used for immobilization of the pincer–metal complexes without affecting the catalytic activity of the individual sites. The application of a number of shape-persistent nanosize $(NCN–Pd^{II})_n$ complexes (**7**, $n = 3$; **8**, $n = 3$; **9**, $n = 8$; **10**, $n = 12$) as homogeneous catalysts in the same Michael reaction, confirmed this expectation. For complexes **7**, **8** and **9**, the catalytic activity per Pd^{II} center was found to be the same as for the monopincer analogs. Only dodecakis(NCN–Pd^{II}) complex **10** showed an almost threefold enhancement in catalytic activity per Pd^{II} center, which is ascribed to the high catalyst concentration at the periphery of this material.

Introduction

Metalated pincer complexes (see Figure 1) have been successfully applied as homogeneous catalysts in organic transformations.[1] Advantageous to the pincer system is the ease of alteration of several functionalities, allowing fine-tuning of these pincer complexes for the desired application.[2] The donor substituents Y can be varied easily, giving access to NCN- (Y = NR'_2), PCP- (Y = PR'_2) and SCS-type (Y = SR′) pincer ligands. As a result, metal centers such as palladium, platinum, nickel, iridium, ruthenium and rhodium can nowadays be introduced into the various pincer ligands thereby allowing application of pincer catalysts in a broad range of catalytic reactions.[2] Furthermore, chirality can be introduced into the pincer catalysts by the benzylic substituent R′′ and/or the donor group Y, opening the possibility for asymmetric catalysis.[3] In addition, the electronic as well as the steric environment of the metal center can be fine-tuned by variation of the substituent Y and/or the R′ groups attached to Y. A recent study illustrated the influence of the donor substituent Y on the catalytic activity of cationic YCY−Pd^{II} complexes in a double Michael reaction.[4] It was found that NCN-type catalysts were superior to SCS- and PCP-type catalysts, while also small effects on the catalytic activity were observed when different types of N-donor groups were used. Finally, the *para* substituent R (Figure 1) can also be used to influence the electron density at the metal center. An illustrative example of the *para* substituent influence on the reactivity of a pincer−metal catalyst was reported by Van de Kuil et al., in which various *para*-substituted NCN−Ni^{II} catalysts were studied in the Kharasch addition reaction.[1d,5] Electron-donating and -withdrawing substituents were found to have a significant effect on the Ni^{II}/Ni^{III} oxidation potential, the crucial step in the catalytic cycle of the Kharasch addition.

[a] Debye Institute, Department of Metal-Mediated Synthesis, Utrecht University,
Padualaan 8, 3584 CH Utrecht
Fax: (internat.) + 31-30/2523615
E-mail: g.vankoten@chem.uu.nl
[b] Bijvoet Center for Biomolecular Research, Department of Crystal and Structural Chemistry, Utrecht University,
Padualaan 8, 3584 CH Utrecht
E-mail: a.l.spek@chem.uu.nl
[c] Debye Institute, Department of Theoretical Chemistry, Utrecht University,
Padualaan 14, 3584 CH Utrecht, The Netherlands
E-mail: w.m.klopper@chem.uu.nl
[‡] Correspondence pertaining to crystallographic studies should be addressed to this author.
[‡‡] Correspondence pertaining to theoretical studies should be addressed to this author.

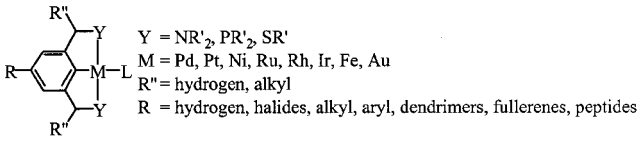

Figure 1. The metalated pincer system

Immobilization of pincer catalysts on soluble or solid supports in order to prepare recyclable catalysts has been intensively studied in recent years.[1e,6] It was demonstrated that the *para* position (R, Figure 1) is excellent for anchoring these pincer complexes to support materials. In particular, we studied shape-persistent multi(YCY−metal) complexes as homogeneous catalysts as well as their application in a nanofiltration membrane reactor in order to enhance total turnover numbers of the catalysts by recycling.[4,7,8] In this field of research, it is desirable to be able to use diverse functionalities at the *para* position of the pincer complex for anchoring purposes. In order to estimate beforehand any uncontrolled influences by these functionalities on the catalytic properties of the pincer−metal moieties, we set out to study the electronic influence of *para* substituents on the catalytic activity of pincer systems in organic transformations. Since (NCN−Pd^{II}) complexes were already found to be very active as homogeneous Lewis acid catalysts in the double Michael reaction between methyl vinyl ketone (MVK) and ethyl α-cyanoacetate[4] and because the conditions nicely meet the requirements for the commercially available nanofiltration membranes,[9] we decided to use this reaction for our catalyst screening. A number of *para*-functionalized, cationic NCN−Pd^{II} complexes [Figure 2, X = $OH_2(BF_4)$] were prepared and applied as Lewis acid catalysts in the double Michael reaction. We also performed density functional theory (DFT) calculations on these systems in order to gain insight in the electronic influence of the *para* substituent on the Pd^{II} center. Furthermore, palladated shape-persistent multi(NCN-pincer) complexes, in which the pincer moiety is anchored to the various supports by different *para* functionalities, were also included in this study.

Results and Discussion

Synthesis of *para*-Substituted NCN−Pd^{II} Complexes

para-Substituted NCN-pincer complexes **1a**−**g** were selected for this study (Figure 2). Complexes **1a** (X = Br),[10] **1b** (X = Br)[11] and **1g** (X = Cl)[12] were prepared according

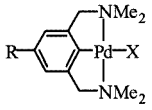

	1a	1b	1c	1d	1e	1f	1g
R	H	NO_2	NMe_2	C(O)Me	OCH_2Ph	Ph	$SiMe_3$

Figure 2. A series of *para*-substituted NCN-pincer palladium(II) complexes

to literature procedures. Palladium(II) complex **1c** (X = Br) was prepared in two steps (Scheme 1). Treatment of *para*-amino pincer derivative **2**[13] with formaldehyde and formic acid, yielded the desired ligand **3c** in 62% yield. Treatment of **3c** with $Pd_2(dba)_3$·$CHCl_3$ in benzene, afforded NCN−palladium(II) complex **1c** (Scheme 1). The *para*-acetyl-substituted NCN-pincer complex **1d** (X = Br) was prepared according to the same palladation procedure, starting from the previously prepared ligand precursor **3d**[13] (Scheme 1).

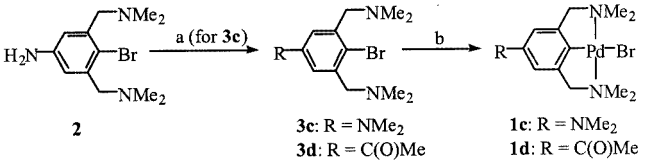

Scheme 1. a) Formaldehyde, formic acid, room temp., 3 h; b) [$Pd_2(dba)_3$]·$CHCl_3$, C_6H_6, room temp., 18 h

para-Benzyloxy pincer complex **1e** (X = I) was synthesized according to a procedure recently developed for the synthesis of nanosize multipincer complexes.[7b] Treatment of a mixture of the *para*-(*tert*-butyldimethylsilyl)-protected phenolic pincer **4**, benzyl bromide, potassium carbonate and 18-crown-6 with tetrabutylammonium fluoride in acetone, resulted in the formation of **1e** in 80% yield (Scheme 2). Note that the metal ion is already present during the introduction step of the *para* substituent, showing the versatility and strength of the pincer system.[14]

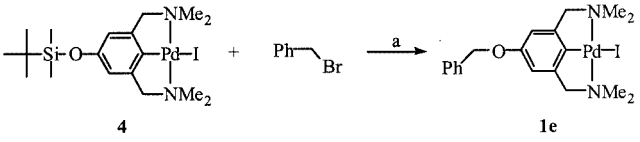

Scheme 2. a) Bu_4NF, K_2CO_3, 18-crown-6, acetone, room temp., 18 h

para-Phenyl pincer complex **1f** (X = Cl) was synthesized from *para*-phenyl-substituted NCN ligand precursor **5**[15] by a lithiation/transpalladation procedure (Scheme 3), affording **1f** in 83% yield.

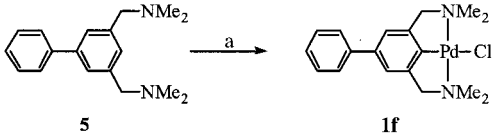

Scheme 3. a) *n*BuLi, hexanes, −80 °C → room temp., 4 h, followed by [$PdCl_2$(cod)], Et_2O, room temp., 2 h

Noteworthy is that three different methods were used to arrive at *para*-substituted NCN−Pd^{II} complexes: i) an oxidative addition reaction (**1a**−**1d**), ii) a lithiation/transmetalation reaction (**1f** and **1g**), and iii) the introduction of the *para* substituent with the metal ion already present in the pincer ligand (**1e**). These examples illustrate the wide variety of reactions which can be used to prepare functionalized pincer−metal complexes. Especially for the synthesis of multi(YCY−metal) complexes, having a variety of

methods available to construct the multimetallic material is considered of great importance.[4,7]

The neutral NCN−Pd^{II} complexes **1a**−**g** were readily converted into the corresponding cationic species **6a**−**g**, the Lewis acid catalyst precursors for the double Michael reaction, by treatment with silver tetrafluoroborate in wet acetone (Scheme 4).[16]

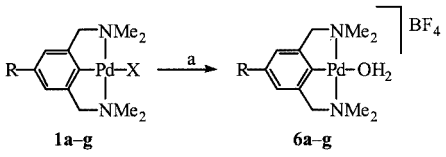

1a–g **6a–g**

Scheme 4. a) $AgBF_4$, wet acetone, room temp., 1 h

Crystals suitable for X-ray crystal structure determination were obtained for neutral NCN−palladium complexes **1c** and **1d** [Figure 3, parts a) and b), respectively]. The molecular structures comprise square-planar palladium(II) centers ligated by a terdentate η^3-coordinating NCN ligand and a bromine ligand *trans* to the aryl ring of the pincer ligand. Table 1 summarizes a number of representative interatomic bond lengths and angles of **1c** and **1d**. The crystal structure of **1d** contains two independent molecules, of which only one is shown in Figure 3. The two molecules differ only slightly in the conformation of the acetyl substituent with respect to the pincer−palladium fragment. In both **1c** and **1d**, the *para* substituents are almost in the same plane with the pincer aryl ring, as can be concluded from the dihedral angles given in Table 1. This coplanarity is commonly observed in the crystal structures of molecules containing an Me_2N−aryl or MeC(O)−aryl moiety.[17] Furthermore, as indicated by the small differences in the Pd−Br distances [**1b**: Pd−Br = 2.5516(3) Å],[11] the different *para* substituents have only minor influences on the electron density of the palladium center.

Density Functional Theory (DFT) Calculations

To further investigate the electronic influences of the *para* substituents on the Lewis acidity of the palladium(II) center, DFT calculations were performed on cationic catalyst precursors **6a**−**g**. Recently, similar calculations on substituted

Table 1. Interatomic distancess [Å] and angles [°] of **1c** and **1d**

1c		**1d**[a]	
Bond lengths:			
Pd1-C1	1.921(2)	Pd1A−C1A	1.911(5)
Pd1−Br1	2.5565(3)	Pd1A−Br1A	2.5636(7)
Pd1−N1	2.119(2)	Pd1A−N1A	2.121(4)
Pd1−N2	2.1171(19)	Pd1A−N2A	2.120(4)
C4−N3	1.387(3)	C6A−C7A	1.499(7)
Bond angles:			
C1−Pd1−Br1	176.99(7)	C1A−Pd1A−Br1A	172.98(15)
C1−Pd1−N1	80.32(9)	C1A−Pd1A−N1A	82.02(19)
C1−Pd1−N2	81.16(9)	C1A−Pd1A−N2A	81.98(18)
N1−Pd1−N2	161.45(7)	N1A−Pd1A−N2A	161.80(16)
Dihedral Angles:			
C14−N3−C4−C5	179.6(2)	C5A−C6A−C7A−O1A	167.6(5)

[a] Only the values for one of the two independent molecules are given.

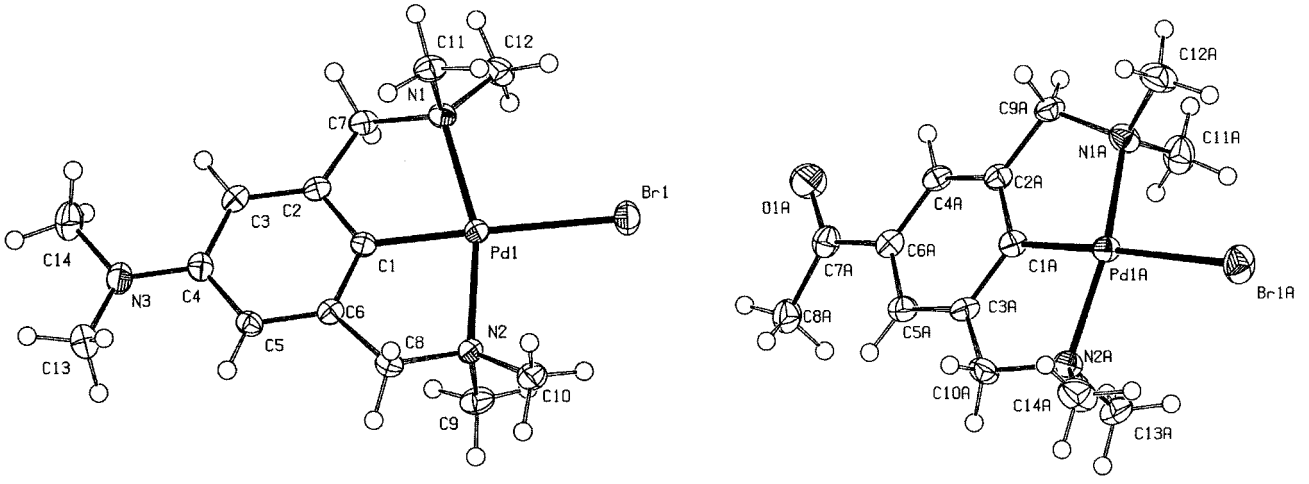

Figure 3. Crystal structures of *para*-substituted NCNPdBr complexes; ORTEP 50% displacement ellipsoids; a) (left): Me_2N−NCNPdBr (**1c**); b) (right): one of the two independent molecules of MeC(O)−NCNPdBr (**1d**)

Table 2. Selected data obtained from DFT calculation with **6a**−**g**, $[R-NCN-Pd(OH_2)]^+$

p-R	Compound	Charge Pd [e][a]	Pd−OH_2 [Å]	Pd−C_{ipso} [Å]	σ_p [b]
H	**6a**	0.187	2.286	1.942	0
NO_2	**6b**	0.217	2.273	1.938	0.778
NMe_2	**6c**	0.171	2.293	1.940	−0.83
C(O)Me	**6d**	0.195	2.281	1.939	0.502
OCH_2Ph	**6e**	0.183	2.286	1.941	−0.42
Ph	**6f**	0.179	2.286	1.940	−0.01
$SiMe_3$	**6g**	0.183	2.285	1.941	−0.07

[a] By means of Mulliken population analysis. [b] Hammett parameters for the various *para*-substituents obtained from Exner.[20]

NCN−Pt^{II} complexes demonstrated that the calculated structures correlated well with the experimental observations.[11b] In addition, the calculated Mulliken charge at the Pt^{II} centers showed a linear relationship with the chemical shifts of the Pt nuclei in the ^{195}Pt NMR spectra of the various complexes as well as with the σ_p Hammett parameter of the various *para* substituents.[11b] The DFT method B3LYP/LANL2DZ[18] as implemented in Gaussian 98[19] was used to calculate the partial charge, by means of Mulliken population analysis, at the palladium(II) centers of *para*-substituted catalyst precursors **6a**−**g**. Table 2 summarizes a number of selected data which were obtained from these calculations and also displays the Hammett parameter (σ_p) of the various *para* substituents.

Both from the Mulliken charge at the Pd^{II} centers and from the Pd−OH_2 and Pd−C_{ipso}(aryl) distances, it becomes clear that the *para* substituent R has only a minor electronic influence on the palladium(II) center, and thus on its Lewis acidity. Nevertheless, the complexes with the highest Mulliken charge at the Pd^{II} center (**6b** and **6d**, most electron-withdrawing substituents) have the shortest calculated Pd−O distances, while complex **6c** (most electron-donating substituent) possessing the lowest Mulliken charge at the Pd^{II} center displays the largest Pd−O distance (Table 2). In addition, plotting the Hammett parameter (σ_p) against the calculated Mulliken charge at the Pd^{II} centers of **6a**−**g**, clearly demonstrates the expected trend (Figure 4). Although, the linear fit is rather poor (in particular **6b** shows a significant deviation), this result indicates that DFT calculations can be used to predict the relative electronic influence of substituents on catalytically active metal centers.

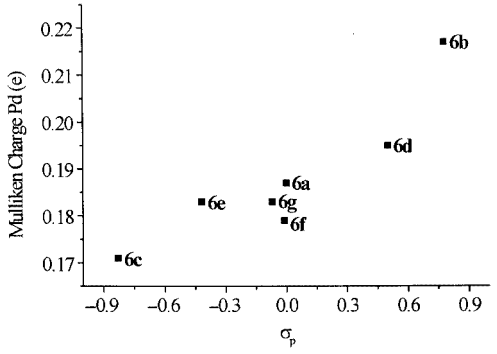

Figure 4. Linear relationship between Hammett parameter (σ_p) of the *para* substituents and Mulliken charge at the Pd centers

Catalysis Using *para*-Substituted NCN−Pd^{II} Catalysts

Cationic NCN−Pd^{II}−aqua complexes **6a**−**g** were applied as homogeneous Lewis acid catalysts in the double Michael reaction between methyl vinyl ketone (MVK) and ethyl α-cyanoacetate (Scheme 5). The results are summarized in Table 3.[21] In all cases 0.5 mol % [Pd^{II}] centers was used. From the $k_{obsd.}$ found for the various catalysts, it is apparent once again that the *para* substituents exert only a small influence on the catalytic activity of the Pd^{II} centers for this particular reaction. Only **6c** (R = Me_2N, Table 3) displays a significantly lower activity in this reaction as compared to the other catalysts.

Table 3. Catalytic results of **6a**−**g** in the double Michael reaction

Catalyst	*p*-R	$k_{obsd.}$ [$\times 10^{-4}$ s^{-1}][a]	$t_{1/2}$ [min][b]
6a	H	2.8	41
6b	NO_2	2.2	53
6c	NMe_2	1.3	89
6d	C(O)Me	2.3	50
6e	OCH_2Ph	2.4	48
6f	Ph	2.7	43
6g	$SiMe_3$	2.6	44

[a] Determined by ^1H NMR spectroscopy by comparison of the integration of the α-CH_2 protons of ethyl α-cyanoacetate to the combined integration of the ethyl ester CH_2 protons of the reactant and product. First-order reactions CN (CN = ethyl α-cyanoacetate); rate constant *k* was determined by plotting $-\ln([CN]/[CN]_0)$ versus time [s]. [b] $t_{1/2} = \ln 2/(k \times 60)$.

Comparison of the experimentally obtained catalytic data with the theoretical data reveals that there is no linear relationship between the observed rate constants ($k_{obsd.}$, Table 3) and the calculated Mulliken charges at the Pd^{II} centers of **6a**−**g** (Table 2). Plotting the Hammett σ_p parameters of the various *para* substituents against the log-

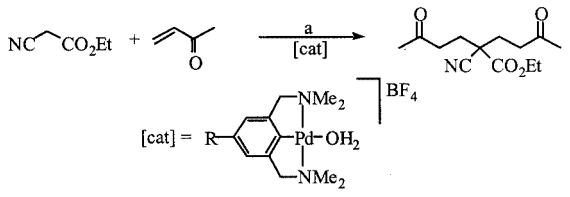

Scheme 5. Double Michael reaction between MVK and ethyl α-cyanoacetate; a) iPr_2NEt (10 mol %), [cat] (0.5 mol %), CH_2Cl_2, room temp.

($k_{obsd.}$) values of **6a**−**g** resulted in a curved function passing through a maximum (Figure 5). This type of behavior has previously been observed for reactions in which a reversible step is followed by an irreversible step.[22] Apparently, the *para* substituents alter the relative magnitude of the rate constants of the individual mechanistic steps and thus change the rate-determining step. In the double Michael reaction, a reversible step − deprotonation of the α-CH_2 group of ethyl α-cyanoacetate − is followed by an irreversible step − the 1,4-addition of the ethyl α-cyanoacetate anion to MVK. Thus, changing the *para* substituent from an electron-withdrawing to an electron-donating group can shift the rate-determining step from the deprotonation step to the nucleophilic 1,4-addition step. From the catalytic data presented in Table 3, it seems that the *p*-NMe_2 substituent has the largest influence, as the activity of **6c** was found to be considerably lower than that of the other catalytic species. Further research to elucidate this change in the rate-determining step is currently under investigation.

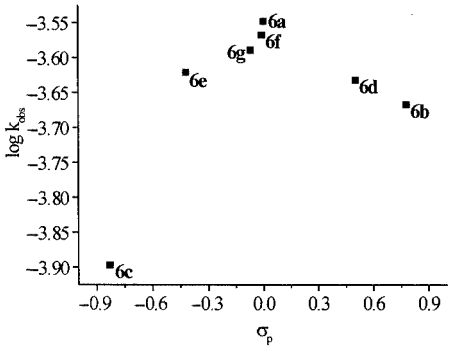

Figure 5. Hammett σ_p parameter versus log($k_{obsd.}$) of **6a**−**g**

Catalysis Using Multi(NCN−Pd^{II}) Catalysts

Previously, we reported the synthesis of shape-persistent multi(NCN−Pd^{II}) catalyst precursors **7**−**10** (Figure 6).[23] These complexes were also applied as homogeneous catalysts in the double Michael reaction between MVK and ethyl α-cyanoacetate (Scheme 5). The catalytic results are

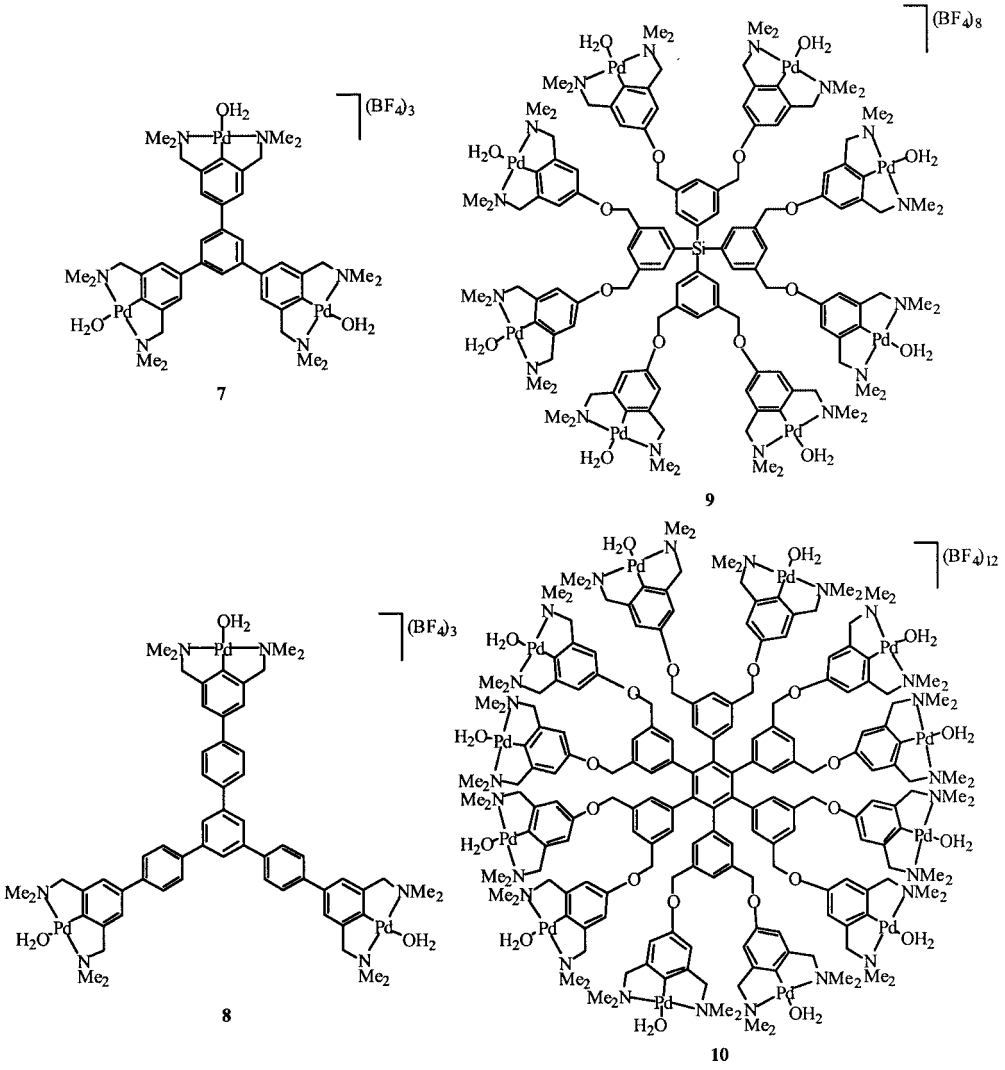

Figure 6. Shape-persistent homogeneous Lewis acid catalysts

Table 4. Catalytic activities of **7**−**10** in the double Michael reaction

Catalyst	$k_{obsd.}$ [$\times 10^{-4}$ s^{-1}][a]	$t_{1/2}$ [min][b]
7	2.3	50
8	2.6	44
9	2.1	55
10	8.1	14

[a] Determined by ^{1}H NMR spectroscopy by comparison of the integration of the α-CH_2 protons of ethyl α-cyanoacetate to the combined integration of the ethyl ester CH_2 protons of the reactant and product. First-order reactions CN (CN = ethyl α-cyanoacetate); rate constant k was determined by plotting $-\ln[CN/[CN]_0)$ versus time [s]. [b] $t_{1/2} = \ln 2/(k \times 60)$.

summarized in Table 4. In all cases, 0.5 mol % [Pd^{II}] centers was used and the $k_{obsd.}$ values for the various multimetallic systems were determined per palladium(II) center.

The catalysis results obtained for the tris(NCN−Pd^{II}) catalyst **7** (Table 4) were reported previously.[4] Compared to the catalytic activity of the reference monometallic catalyst **6a** (R = H, Table 3), it becomes clear that the catalytic activities per palladium(II) center for multi(NCN−Pd^{II}) catalysts **7**−**9** (Table 4) are similar, indicating that all palladium(II) centers in **7**−**9** act as independent catalytic sites. This is an important result; it implies an efficient use of all catalytic sites during catalysis. In addition, it once again underlines that the (Lewis acid) catalytic activity depends little on the *para* functionality of the pincer moiety, which is in agreement with the results obtained for the monometallic *para*-substituted NCN−Pd^{II} catalysts (Table 3). Interestingly, the dodecakis(NCN−Pd^{II}) catalyst **10** shows an almost threefold increase in catalytic activity per Pd^{II} center (Table 4) as compared to reference **6a** (R = H, Table 3). This increase in catalytic activity does not originate from the influence of the *para* substituent, since no increase in catalytic activity was observed for **6e** (R = OCH_2Ph, Table 3) and **9** (Table 4), both possessing the same *para* substituent as **10**. Molecular modeling studies of the isostructural platinum analogs of **9** and **10**,[7b] respectively, already indicated that on average the metal sites are in closer proximity to each other in the case of **10**, suggesting cooperative effects between the Pd^{II} centers during catalysis. Another possible explanation is that large aggregates of **10**, induced by the polar organometallic periphery, assemble in solution, resulting in the formation of polar micro-environments and thereby enhancing the catalytic transformations. This aggregate formation would be more difficult for **9** due to its spherical geometry.

Conclusions

A series of *para*-substituted NCN−Pd^{II} complexes was synthesized and the electronic influence of the *para* substituents on the Lewis-acidic palladium(II) centers was investigated by means of catalysis and DFT calculations. The application of these complexes as homogeneous Lewis acid catalysts in the double Michael reaction between MVK and ethyl α-cyanoacetate, clearly showed that in general the *para* substituents only slightly affect the catalytic activity of the Pd^{II} centers. Only the use of the *para*-(dimethylamino) substituent (**6c**) resulted in a considerable decrease in the catalytic activity. These results were confirmed by DFT calculations, which revealed that the *para* substituents have only minor influences on the partial charge (expressed by the Mulliken population) and thus on the Lewis acidity of the palladium(II) centers. In addition, several shape-persistent multi(NCN−Pd^{II}) complexes were applied as Lewis acid catalysts in the double Michael reaction. The catalysis results of **7**−**9** showed that all catalytic sites act as independent catalysts; the activities per Pd^{II} center were similar to the activities found for the mononuclear catalysts. Surprisingly, the dodecakis(NCN−Pd^{II}) system **10** exhibited a threefold increase in catalytic activity, probably due to cooperativity between metalated pincer groups at the periphery of **10**. Retention measurements with the isostructural platinum analogs of **7**−**10** in a nanofiltration membrane reactor have already shown that these shape-persistent complexes are very efficiently retained by nanofiltration membranes.[7b] Currently, these shape-persistent nanosize complexes are being further explored as homogeneous catalysts in a nanofiltration membrane reactor under continuously operating conditions.

Experimental Section

General: Solvents were purified and dried according to standard procedures, stored under nitrogen and freshly distilled prior to use. NMR solvents were purchased and used without further purification. Compounds **1a**,[10] **1b**,[11] **1g**,[12] **2**,[1d] **3d**,[5] **4**,[7b] **5**,[15] **6a**,[16] and [$PdCl_2$(cod)][24] were prepared according to literature procedures. All other reagents were purchased and used without further purification. NMR spectra were recorded with a Varian 300 spectrometer (^{1}H NMR: 300.1 MHz. ^{13}C NMR: 75.5 MHz. ^{31}P NMR: 121.5 MHz) or a Varian Gemini 200 spectrometer (^{1}H NMR: 200.1 MHz. ^{13}C NMR: 50.3 MHz. ^{31}P NMR: 81.0 MHz). Microanalyses were determined by Dornis and Kolbe, Mikroanalytisches Laboratorium, Mülheim a. d. Ruhr, Germany.

3c: Arylamine **2** (0.20 g, 0.68 mmol) was dissolved in a mixture of formaldehyde (10 mL) and formic acid (10 mL) and this mixture was stirred at room temperature for 3 h. Subsequently, 1 M NaOH (aq) was added to this solution until pH = 11 was reached. The aqueous layer was extracted with CH_2Cl_2 (3 × 20 mL) and the combined organic layers were dried with $MgSO_4$. After evaporation of all volatiles, hexanes (20 mL) were added and the resulting mixture was filtered and the solvents were evaporated to dryness, leaving a slightly brown solid. This product was used without further purification. Yield: 0.13 g (62%). ^{1}H NMR ($CDCl_3$, 200 MHz): δ = 2.30 (s, 12 H, NCH_3), 2.95 (s, 6 H, *p*-NCH_3), 3.50 (s, 4 H, CH_2), 6.74 (s, 2 H, Ar*H*) ppm. ^{13}C NMR ($CDCl_3$, 75 MHz): δ = 40.95, 45.98, 64.49, 114.15, 123.66, 138.77, 149.59 ppm.

1c: [Pd_2(dba)$_3$]·$CHCl_3$ (0.33 g, 0.32 mmol) in benzene (10 mL) was added to a solution of **3c** (0.20 g, 0.64 mmol) in benzene (10 mL) and this solution was stirred at room temperature for 3 h. Subsequently, all volatiles were evaporated, CH_2Cl_2 (15 mL) was added and the resulting solution was filtered through Celite. The Celite layer was washed with CH_2Cl_2 (2 × 5 mL). The combined filtrates

were concentrated to ca. 5 mL and upon addition of Et_2O (10 mL) the product precipitated from the yellow solution. Light-brown crystals suitable for a crystal structure determination were obtained by slow diffusion of pentane into a concentrated solution of **1c** in CH_2Cl_2. Yield: 0.13 g (50%). ^1H NMR ($CDCl_3$, 200 MHz): δ = 2.86 (s, 6 H, *p*-NCH_3), 2.96 (s, 12 H, NCH_3), 3.95 (s, 4 H, CH_2), 6.26 (s, 2 H, Ar*H*) ppm. ^{13}C NMR ($CDCl_3$, 75 MHz): δ = 41.55, 53.96, 75.05, 105.28, 144.53, 145.67, 149.53 ppm. $C_{14}H_{24}BrN_3Pd$ (420.69): calcd. C 39.97, H 5.75, N 9.99; found C 39.78, H 5.67, N 9.92.

1d: Synthesis as described for **1c**, using **3d** (0.20 g, 0.64 mmol) and $Pd_2(dba)_3{\cdot}CHCl_3$ (0.33 g, 0.32 mmol) in benzene (10 mL). Orange/brown crystals of **1d** suitable for a crystal structure determination were obtained by slow concentration in air of a concentrated solution of **1d** in CH_2Cl_2. Yield: 0.18 g (67%). ^1H NMR ($CDCl_3$, 200 MHz): δ = 2.52 [s, 3 H, C(O)CH_3], 2.99 (s, 12 H, NCH_3), 4.05 (s, 4 H, NCH_2), 7.41 (s, 2 H, Ar*H*) ppm. ^{13}C NMR ($CDCl_3$, 75 MHz): δ = 26.80, 54.09, 74.66, 120.22, 134.75, 145.45, 197.92 ppm. $C_{14}H_{21}BrN_2OPd$ (419.66): calcd. C 40.07, H 5.04, N 6.68; found C 40.26, H 5.11, N 6.56.

1e: Tetrabutylammonium fluoride (1 M in THF) (0.54 mL, 0.54 mmol) was added to a mixture of **4** (0.30 g, 0.54 mmol), benzyl bromide (0.10 mL, 0.83 mmol), K_2CO_3 (0.38 g, 2.7 mmol) and 18-crown-6 (13 mg, 0.05 mmol) in acetone (15 mL). This mixture was stirred at room temperature for 5 h. Subsequently, all volatiles were evaporated, CH_2Cl_2 (15 mL) was added and the resulting mixture was filtered. The filtrate was reduced to 5 mL and upon addition of Et_2O (10 mL) the product precipitated as an off-white solid. Slow diffusion of Et_2O into a concentrated solution of **1e** in CH_2Cl_2, afforded analytically pure **1e** as a white powder. Yield: 0.17 g (59%). ^1H NMR ($CDCl_3$, 300 MHz): δ = 2.98 (s, 12 H, NCH_3), 3.97 (s, 4 H, NCH_2), 4.98 (s, 2 H, OCH_2), 6.49 (s, 2 H, Ar*H*), 7.30−7.42 (m, 5 H, Ar*H*) ppm. ^{13}C NMR ($CDCl_3$, 75 MHz): δ = 54.01, 73.66, 74.80, 107.25, 127.65, 128.22, 128.84, 137.32, 145.86, 157.48 ppm. $C_{19}H_{25}IN_2OPd$ (530.74): calcd. C 43.00, H 4.75, N 5.28; found C 43.15, H 4.80, N 5.24.

1f: *n*BuLi (2.3 mL, 3.7 mmol) was added to a solution of **5** (1.0 g, 3.7 mmol) in dry hexanes (20 mL) at −80 °C. After the addition was completed, the temperature was allowed to rise to room temperature and stirring was continued for 4 h. Subsequently, this solution was added to a suspension of [$PdCl_2$(cod)] (1.1 g, 3.7 mmol) in Et_2O at room temperature and the resulting mixture was stirred for an additional 3 h. The solvents were evaporated to dryness and the residue was extracted with CH_2Cl_2 (10 mL). The organic layer was filtered through Celite and the filtrate was reduced to ca. 3 mL. Addition of Et_2O resulted in the formation of a white precipitate which was collected and dried in vacuo. Analytically pure **1f** was obtained by slow diffusion of Et_2O into a concentrated solution of **1f** in CH_2Cl_2, affording colorless needles of **1f**. Yield: 1.2 g (78%). ^1H NMR ($CDCl_3$, 200 MHz): δ = 2.97 (s, 12 H, NCH_3), 4.05 (s, 4 H, NCH_2), 7.00 (s, 2 H, Ar*H*), 7.30−7.51 (m, 5 H, Ar*H*) ppm. ^{13}C NMR ($CDCl_3$, 75 MHz): δ = 53.38 (C_{ipso} signal not observed), 75.03, 119.00, 127.16, 128.99, 138.51, 141.84, 145.65, 156.09 ppm. $C_{18}H_{23}ClN_2Pd$ (409.27): calcd. C 52.83, H 5.66, N 6.84; found C 52.65, H 5.75, N 6.73.

General Procedure for the Synthesis of 6a−g: $AgBF_4$ (97.3 mg, 0.50 mmol) in wet acetone (1 mL) was added to a solution of **1a−g** (0.50 mmol) in acetone (10 mL) and the resulting solution was stirred at room temperature for 1 h. The mixture was filtered through Celite and the filtrate was concentrated to ca. 3 mL. Upon slow addition of Et_2O (5 mL), the product precipitated as an off-white solid. After isolation, the product was analyzed by ^1H NMR spectroscopy and immediately used in the catalytic experiments.

6a:[16] Yield: 0.17 g (86%). ^1H NMR ([D_6]acetone, 300 MHz): δ = 2.87 (s, 12 H, NCH_3), 4.11 (s, 4 H, NCH_2), 6.84 (d, $^3J_{H,H}$ = 7.5 Hz, 2 H, Ar*H*), 7.02 (t, $^3J_{H,H}$ = 7.5 Hz, 1 H, Ar*H*) ppm. ^{13}C NMR ([D_6]acetone, 75 MHz): δ = 51.72, 73.32, 120.42, 125.48, 145.68, 150.49 ppm.

6b: Yield: 0.17 g (78%). ^1H NMR ([D_6]acetone, 300 MHz): δ = 2.92 (s, 12 H, NCH_3), 4.34 (s, 4 H, NCH_2), 7.79 (s, 2 H, Ar*H*) ppm. ^{13}C NMR ([D_6]acetone, 75 MHz): δ = 51.93, 73.08, 115.81, 146.80, 146.90, 161.97 ppm.

6c: Yield: 0.15 g (67%). ^1H NMR ([D_6]acetone, 200 MHz): δ = 2.81 (s, 6 H, *p*-NCH_3), 2.83 (s, 12 H, NCH_3), 4.08 (s, 4 H, NCH_2), 6.38 (s, 2 H, Ar*H*) ppm.

6d: Yield: 0.21 g (93%). ^1H NMR ([D_6]acetone, 300 MHz): δ = 2.49 [s, 3 H, C(O)CH_3], 2.94 (s, 12 H, NCH_3), 4.22 (s, 4 H, NCH_2), 7.50 (s, 2 H, Ar*H*) ppm. ^{13}C NMR ([D_6]acetone, 75 MHz): δ = 26.02, 52.42, 73.66, 120.42, 135.78, 146.80, 162.29, 197.02 ppm.

6e: Yield: 0.24 g (95%). ^1H NMR ([D_6]acetone, 300 MHz): δ = 2.85 (s, 12 H, NCH_3), 4.13 (s, 4 H, NCH_2), 5.04 (s, 2 H, OCH_2), 6.63 (s, 2 H, Ar*H*), 7.32−7.46 (m, 5 H, Ar*H*) ppm. ^{13}C NMR ([D_6]acetone, 75 MHz): δ = 52.01, 70.13, 73.49, 107.80, 127.71, 127.95, 128.61, 137.83, 146.11, 158.28 ppm.

6f: Yield: 0.22 g (93%). ^1H NMR ([D_6]acetone, 300 MHz): δ = 2.89 (s, 12 H, NCH_3), 4.25 (s, 4 H, NCH_2), 7.18 (s, 2 H, Ar*H*), 7.29−7.60 (m, 5 H, Ar*H*) ppm. ^{13}C NMR ([D_6]acetone, 75 MHz): δ = 51.93, 73.45, 119.29, 129.06, 126.94, 127.24, 139.08, 141.54, 146.13, 150.31 ppm.

6g: Yield: 0.22 g (91%). ^1H NMR ([D_6]acetone, 200 MHz): δ = 0.21 (s, 9 H, SiCH_3), 2.85 (s, 12 H, NCH_3), 4.16 (s, 4 H, NCH_2), 7.03 (s, 2 H, Ar*H*) ppm. ^{13}C NMR ([D_6]acetone, 75 MHz): δ = −1.48, 51.84, 73.45, 125.07, 136.92, 145.30, 152.75 ppm.

Catalysis in the Double Michael Reaction Between MVK and Ethyl α-Cyanoacetate. A Typical Experiment. Ethyl α-cyanoacetate (0.17 mL, 1.6 mmol), methyl vinyl ketone (0.40 mL, 4.8 mmol), ethyldiisopropylamine (28 μL, 0.16 mmol) and **6a** (3.2 mg, 8 μmol, 0.5 mol % [Pd]) were mixed in CH_2Cl_2 (5 mL) and stirred at room temperature. The reaction mixture was sampled (100 μL) at regular intervals and the samples worked up by evaporating solvent and methyl vinyl ketone with a gentle stream of nitrogen. The conversions were determined by ^1H NMR spectroscopy. Conversions obtained were confirmed by GC analysis of the reaction mixture. In all cases, the product was isolated by bulb-to-bulb distillation. For all reactions, yields were found to be between 85 and 100%.

Crystal Structure Determinations: Intensities were measured with a Nonius KappaCCD diffractometer with rotating anode (Mo-K_α, λ = 0.71073 Å) at a temperature of 150 K. The structure was solved with automated Patterson methods using the program DIRDIF97,[25] and refined with the program SHELXL-97[26] against F^2 of all reflections up to a resolution of $(\sin/\lambda)_{max}$ = 0.65 $Å^{-1}$. Non-hydrogen atoms were refined freely with anisotropic displacement parameters. Hydrogen atoms were refined as rigid groups. The drawings, structure calculations, and checking for higher symmetry was performed with the program PLATON.[27]

Compound 1c: $C_{14}H_{24}BrN_3Pd$, M = 420.67, orange plate, 0.24 × 0.24 × 0.09 mm, monoclinic, $P2_1/c$ (no. 14), a = 9.1973(1) Å, b = 11.1707(2) Å, c = 16.4736(3) Å, β = 108.3990(8)°, V = 1605.98(4) $Å^3$, Z = 4, ρ = 1.740 g cm^{-3}. The absorption correction was per-

formed with PLATON[27] (routine DELABS, μ = 3.64 mm^{-1}, 0.49−0.72 transmission). 17563 measured reflections, 3671 unique reflections (R_{int} = 0.0508), 2999 observed reflections [$I > 2\sigma(I)$]. 178 refined parameters, 0 restraints. *R* (obsd. refl.): *R*1 = 0.0254, *wR*2 = 0.0517. *R* (all data): *R*1 = 0.0387, *wR*2 = 0.0549. *S* = 1.039. CCDC-187019 contains the supplementary crystallographic data for this paper. These data can be obtained free of charge at www.ccdc.cam.ac.uk/conts/retrieving.html [or from the Cambridge Crystallographic Data Centre, 12 Union Road, Cambridge CB2 1EZ, UK; Fax: (internat.) + 44-1223/336-033; E-mail: deposit@ccdc.cam.ac.uk].

Compound 1d: $C_{14}H_{21}BrN_2OPd$, *M* = 419.64, yellow plate, 0.12 × 0.12 × 0.05 mm, monoclinic, $P2_1/c$ (no. 14), *a* = 17.1168(3) Å, *b* = 15.1078(3) Å, *c* = 12.4777(3) Å, β = 107.1925(12)°, *V* = 3082.52(11) $Å^3$, *Z* = 8, ρ = 1.808 g cm^{-3}. The absorption correction was performed with PLATON[27] (routine MULABS, μ = 3.79 mm^{-1}, 0.68−0.82 transmission). 26887 measured reflections, 7047 unique reflections (R_{int} = 0.0729), 5091 observed reflections [$I > 2\sigma(I)$]. 353 refined parameters, 0 restraints. *R* (obsd. refl.): *R*1 = 0.0456, *wR*2 = 0.0931. *R* (all data): *R*1 = 0.0748, *wR*2 = 0.1034. *S* = 1.012. CCDC-187020 contains the supplementary crystallographic data for this paper. These data can be obtained free of charge at www.ccdc.cam.ac.uk/conts/retrieving.html [or from the Cambridge Crystallographic Data Centre, 12 Union Road, Cambridge CB2 1EZ, UK; Fax: (internat.) + 44-1223/336-033; E-mail: deposit@ccdc.cam.ac.uk].

Acknowledgments

This work was supported by the Council for Chemical Sciences of the Netherlands Organization for Scientific Research (CW/NWO) and the Dutch Technology Foundation (STW).

[1] For representative examples see: [1a] M. Gupta, C. Hagen, R. J. Flesher, W. C. Kaska, C. M. Jensen, *Chem. Commun.* **1996**, 2083−2084. [1b] P. Dani, T. Karlen, R. A. Gossage, S. Gladiali, G. van Koten, *Angew. Chem. Int. Ed.* **2000**, *39*, 743−745; *Angew. Chem.* **2000**, *112*, 759−761. [1c] M. Ohff, A. Ohff, M. E. van der Boom, D. Milstein, *J. Am. Chem. Soc.* **1997**, *119*, 11687−11688. [1d] L. A. van de Kuil, D. M. Grove, R. A. Gossage, J. W. Zwikker, L. W. Jenneskens, W. Drenth, G. van Koten, *Organometallics* **1997**, *16*, 4985−4994. [1e] D. E. Bergbreiter, P. L. Osburn, Y.-S. Liu, *J. Am. Chem. Soc.* **1999**, *121*, 9531−9538. [1f] A. S. Gruber, D. Zim, G. Ebeling, A. L. Monteiro, J. Dupont, *Org. Lett.* **2000**, *2*, 1287−1290. [1g] C. Granel, Ph. Dubois, R. Jérôme, Ph. Teyssié, *Macromolecules* **1996**, *29*, 8576−8582.

[2] For a review about pincer−metal(d^8) chemistry see; M. Albrecht, G. van Koten, *Angew. Chem. Int. Ed.* **2001**, *40*, 3750−3781; *Angew. Chem.* **2001**, *113*, 3866−3898.

[3] [3a] F. Gorla, A. Togni, L. M. Venanzi, A. Albinati, F. Lianza, *Organometallics* **1994**, *13*, 1607−1616. [3b] J. M. Longmire, X. Zhang, M. Shang, *Organometallics* **1998**, *17*, 4374−4379. [3c] M. A. Stark, G. Jones, C. J. Richards, *Organometallics* **2000**, *19*, 1282−1291. [3d] Y. Motoyama, H. Narusawa, H. Nishiyama, *Chem. Commun.* **1999**, 131−132. [3e] S. E. Denmark, R. A. Stavenger, A.-M. Faucher, J. P. Edwards, *J. Org. Chem.* **1997**, *62*, 3375−3385. [3f] L. A. van de Kuil, Y. S. J. Veldhuizen, D. M. Grove, J. W. Zwikker, L. W. Jenneskens, W. Drenth, W. J. J. Smeets, A. L. Spek, G. van Koten, *Recl. Trav. Chim. Pays-Bas* **1994**, *113*, 267−277. [3g] M. Albrecht, B. M. Kocks, A. L. Spek, G. van Koten, *J. Organomet. Chem.* **2001**, *624*, 271−286. [3h] B. S. Williams, P. Dani, M. Lutz, A. L. Spek, G. van Koten, *Helv. Chim. Acta* **2001**, *84*, 3519−3530.

[4] H. P. Dijkstra, M. D. Meijer, J. Patel, R. Kreiter, G. P. M. van Klink, M. Lutz, A. L. Spek, A. J. Canty, G. van Koten, *Organometallics* **2001**, *20*, 3159−3168.

[5] L. A. van de Kuil, H. Luitjes, D. M. Grove, J. W. Zwikker, J. G. M. van der Linden, A. M. Roelofsen, L. W. Jenneskens, W. Drenth, G. van Koten, *Organometallics* **1994**, *13*, 468−477.

[6] [6a] J. W. J. Knapen, A. W. van der Made, J. C. de Wilde, P. W. N. M. van Leeuwen, P. Wijkens, D. M. Grove, G. van Koten, *Nature* **1994**, *372*, 659−663. [6b] A. W. Kleij, R. A. Gossage, R. J. M. Klein Gebbink, E. J. Reyerse, N. Brinkmann, U. Kragl, M. Lutz, A. L. Spek, G. van Koten, *J. Am. Chem. Soc.* **2000**, *122*, 12112−12124. [6c] M. Albrecht, N. J. Hovestad, J. Boersma, G. van Koten, *Chem. Eur. J.* **2001**, *7*, 1289−1294. [6d] P. J. Davies, D. M. Grove, G. van Koten, *Organometallics* **1997**, *16*, 800−802. [6e] M. Albrecht, R. A. Gossage, M. Lutz, A. L. Spek, G. van Koten, *Chem. Eur. J.* **2000**, *6*, 1431−1445. [6f] M. D. Meijer, N. Ronde, D. Vogt, G. P. M. van Klink, G. van Koten, *Organometallics* **2001**, *20*, 3993−4000. [6g] L. A. van de Kuil, D. M. Grove, J. W. Zwikker, L. W. Jenneskens, W. Drenth, G. van Koten, *Chem. Mater.* **1994**, *6*, 1675−1683. [6h] C. Patmamanoharan, P. Wijkens, D. M. Grove, A. P. Philipse, *Langmuir* **1996**, *12*, 4372−4377.

[7] [7a] H. P. Dijkstra, P. Steenwinkel, D. M. Grove, M. Lutz, A. L. Spek, G. van Koten, *Angew. Chem. Int. Ed.* **1999**, *38*, 2186−2188; *Angew. Chem.* **1999**, *111*, 2321−2324. [7b] H. P. Dijkstra, C. A. Kruithof, N. Ronde, R. van de Coevering, D. J. Ramón, D. Vogt, G. P. M. van Klink, G. van Koten, *J. Org. Chem.*, in press, manuscript available on the world wide web: http://pubs3.acs.org/acs/journals. [7c] H. P. Dijkstra, M. Albrecht, G. van Koten, *Chem. Commun.* **2002**, 126−127.

[8] For an overview on homogeneous catalyst recycling using ultra- and nanofiltration membranes see: H. P. Dijkstra, G. P. M. van Klink, G. van Koten, *Acc. Chem. Res.* **2002**, *35*, 798−810.

[9] See ref.[7b] SelRo-nanofiltration membranes (MPF-60: MWCO = 400 Dalton; MPF-50: MWCO = 700 Dalton) were purchased from Koch Membrane Systems Inc., Düsseldorf, Germany; further product information can be found at http://www.kochmembrane.com.

[10] P. L. Alsters, P. J. Baesjou, M. D. Janssen, H. Kooijman, A. Sicherer-Roetman, A. L. Spek, G. van Koten, *Organometallics* **1992**, *11*, 4124−4135.

[11] [11a] M. Q. Slagt, R. J. M. Klein Gebbink, G. van Koten, *J. Chem. Soc., Dalton Trans.* **2002**, 2591−2592. [11b] M. Q. Slagt, G. Rodríguez, R. J. M. Klein Gebbink, W. Klopper, M. Lutz, A. L. Spek, G. van Koten, submitted.

[12] A. W. Kleij, H. Kleijn, J. T. B. H. Jastrzebski, A. L. Spek, G. van Koten, *Organometallics* **1999**, *18*, 277−285.

[13] For the synthesis of **2** and **3d**, see ref.[1d] and ref.[5], respectively.

[14] G. Rodríguez, M. Albrecht, J. Schoenmaker, A. Ford, M. Lutz, A. L. Spek, G. van Koten, *J. Am. Chem. Soc.* **2002**, *124*, 5127−5138.

[15] P. Steenwinkel, S. L. James, D. M. Grove, N. Veldman, A. L. Spek, G. van Koten, *Chem. Eur. J.* **1996**, *2*, 1440−1445.

[16] D. M. Grove, G. van Koten, J. N. Louwen, J. G. Noltes, A. L. Spek, H. J. C. J. Ubbels, *J. Am. Chem. Soc.* **1982**, *104*, 6609−6616.

[17] This information can be obtained from the Cambridge Structural Database: F. H. Allen, O. Kennard, *Chem. Des. Autom. News* **1993**, *8*, 1 and 31.

[18] The DFT-B3LYP/LANL2DZ method uses density functional theory combined with effective core potentials. The basis set used for palladium is the Los Alamos National Laboratory set (LANL) for effective core potentials (ECP) of double ζ type, consisting of a small core ECP with 3s and 3p orbitals in the valence space. The functional form used is the B3LYP, and the relativistic correlations for heavy atoms are considered in the ECP.

[19] M. J. Frisch, G. W. Trucks, H. B. Schlegel, G. E. Scuseria, M. A. Robb, J. R. Cheeseman, V. G. Zakrzewski, J. A. Montgomery Jr., R. E. Stratmann, J. C. Burant, S. Dapprich, J. M. Millam, A. D. Daniels, K. N. Kudin, M. C. Strain, O. Farkas, J. Tomasi, V. Barone, M. Cossi, R. Cammi, B. Mennucci, C. Po-

melli, C. Adamo, S. Clifford, J. Ochterski, G. A. Petersson, P. Y. Ayala, Q. Cui, K. Morokuma, D. K. Malick, A. D. Rabuck, K. Raghavachari, J. B. Foresman, J. Cioslowski, J. V. Ortiz, A. G. Baboul, B. B. Stefanov, G. Liu, A. Liashenko, P. Piskorz, I. Komaromi, R. Gomperts, R. L. Martin, D. J. Fox, T. Keith, M. A. Al-Laham, C. Y. Peng, A. Nanayakkara, C. Gonzalez, M. Challacombe, P. M. W. Gill, B. Johnson, W. Chen, M. W. Wong, J. L. Andres, C. Gonzalez, M. Head-Gordon, E. S. Replogle, J. A. Pople, *Gaussian 98*, Revision A.7, Gaussian, Inc., Pittsburgh PA, **1998**.

[20] O. Exner, *Correlation Analysis of Chemical Data*, Plenum Press, New York, **1998**.

[21] The catalytic results obtained for **6a** were previously published; see ref.[4]

[22] J. Shorter in *Correlation Analysis in Organic Chemistry: an Introduction to the Linear Free-energy Relationships*, Clarendon Press, Oxford, **1973**.

[23] For the synthesis of **7**, see ref.[4] For the synthesis of **8**−**10**, see ref.[7b]

[24] D. Drew, J. R. Doyle, A. G. Shaver, *Inorg. Synth.* **1972**, *13*, 47.

[25] P. T. Beurskens, G. Admiraal, G. Beurskens, W. P. Bosman, S. Garcia-Granda, R. O. Gould, J. M. M. Smits, C. Smykalla, *The DIRDIF97 program system*, Technical Report of the Crystallography Laboratory, University of Nijmegen, The Netherlands, **1997**.

[26] G. M. Sheldrick, *SHELXL-97, Program for crystal structure refinement*, University of Göttingen, Germany, **1997**.

[27] A. L. Spek, *PLATON, A multipurpose crystallographic tool*, Utrecht University, The Netherlands, **2002**.

Received September 16, 2002
[I02523]